energies

MDPI

Article

Effect of Pyrolysis Temperature on Chemical Structure and Thermal Stability of Digestate-Based Biochar

Justyna Kujawska [1,*], Wojciech Cel [1], Barbara Charmas [2] and Dorota Szala [3]

[1] Faculty of Environmental and Energy, Lublin University of Technology, Nadbystrzycka 40B, 20-618 Lublin, Poland; w.cel@pollub.pl
[2] Faculty of Chemistry, Maria Curie-Sklodowska University, Maria Curie-Sklodowska 3, 20-031 Lublin, Poland; barbara.charmas@mail.umcs.pl
[3] Faculty of Biology and Biotechnology, Maria Curie-Sklodowska University, Akademicka 19, 20-033 Lublin, Poland; dorotaszalazar@gmail.com
* Correspondence: j.kujawska@pollub.pl

Abstract

Biochar obtained from digestate is a promising material in the context of digestate management. However, it is important to note that the properties of the resulting material are largely dependent on the parameters of the pyrolysis process, with temperature being a particularly significant factor. The objective of this study was to evaluate the impacts of the digestate pyrolysis temperature on the chemical structure, thermal stability, and thermal decomposition characteristics of biochar produced at temperatures of 400, 500, 600, and 800 °C in an inert nitrogen atmosphere. Material characterization was performed using a range of analytical techniques, including elemental analysis, FTIR spectroscopy, thermogravimetric analysis (TGA/DTG), and coupled TGA–FTIR analysis, in order to identify volatile products released during the heating process. The results demonstrated that elevating the pyrolysis temperature results in progressive carbonization and aromatization of the carbon structure. Concurrently, functional groups containing oxygen and hydrogen were eliminated, as evidenced by declines in the H/C and O/C atomic ratios. FTIR analysis confirmed the disappearance of aliphatic and hydroxyl bands, as well as the dominance of aromatic structures and mineral components in biochar subjected to high-temperature treatment. The TGA results demonstrated an enhancement in thermal stability with increasing pyrolysis temperature. Concurrently, the TGA–FTIR analysis revealed a substantial decline in the emission of volatile decomposition products from biochar obtained at temperatures ≥600 °C. Overall, the pyrolysis temperature of digestate determines the utilization potential of the resulting biochar; in particular, low-temperature biochar can be used as a soil amendment and methane fermentation stimulant, while high-temperature biochar can be used for contaminant immobilization in soil and long-term carbon sequestration.

Keywords: biochar; digestate; pyrolysis; thermal stability; FTIR; TGA–FTIR; carbon sequestration

Academic Editor: Mohammed Abushammala

Received: 20 January 2026
Revised: 12 February 2026
Accepted: 14 February 2026
Published: 16 February 2026

1. Introduction

Biochar, which is produced by subjecting biomass to pyrolysis under oxygen-limited conditions, has attracted interest due to the possibility of effectively managing organic waste in accordance with circular economy principles and the potential to increase the energy efficiency of biomass conversion processes [1]. The physicochemical and chemical properties of biochar—including its chemical structure, mineral content, specific surface

area, porosity, aromaticity, and thermal stability—are largely determined by the parameters of the pyrolysis process, especially the temperature [2].

It has been demonstrated that elevated pyrolysis temperatures are conducive to the formation of micropores, the development of a porous structure, and augmentation of the specific surface area of biochar; however, these processes have also been observed to concomitantly result in decreased process efficiency and augmented ash content [3,4]. The production of biochar at elevated temperatures has been shown to result in materials exhibiting elevated hydrophobicity, a high carbon content, a more ordered carbon layer structure, and enhanced environmental stability and durability [5]. A substantial corpus of research has focused on the subject, and the findings are clear: an increase in the pyrolysis temperature results in increases in the specific surface area [6], pH [7], and carbon content, while simultaneously reducing the nitrogen content [8].

The H/C and O/C molar ratios are significant indicators of structural changes in biochar, which exhibit certain relationships with the pyrolysis temperature. The H/C and O/C ratios can be utilized to evaluate the aromaticity, polarity, and stability of biochar [9]. It is evident that an increase in the pyrolysis temperature generally results in an increase in the carbon content, whilst concurrently leading to decreases in the nitrogen, hydrogen, and oxygen contents [10].

The volume of digestate—a by-product of anaerobic digestion—is escalating with the development of the biogas sector, necessitating the development of effective management strategies; in this context, a potential solution is the conversion of this material into biochar. According to Xu et al., there are currently over 110,000 biogas installations worldwide, with a total biogas production of approximately 12.5×10^{12} m^3 per year [11]. A standard agricultural biogas plant with a capacity of 1 MW processes several dozen Mg of raw materials per day (from 30 to 80 Mg, depending on the energy value of the substrates). The amount of digestate produced, depending on the type of substrate and operating conditions, usually constitutes 70–90% of the input weight [12]. According to forecasts by the European Biogas Association, there is expected to be a substantial increase in global digestate production (expressed in dry matter), which is predicted to rise from approximately 31 Mt DM per year in 2022 to 75 Mt DM per year in 2030 and then to 177 Mt DM per year in 2050 [13].

Digestate is distinguished by its elevated contents of organic matter and essential minerals, including nitrogen, phosphorus, and potassium, rendering it a compelling raw material for subsequent processing [14]. Although it has been recommended for application as an organic fertilizer [15,16], a growing body of research is beginning to shed light on the potential risks associated with the introduction of digestates into soil. As outlined in [17], factors such as intensive nitrate leaching, ammonia, nitrous oxide, volatile organic compounds, and unpleasant odors must be considered. Furthermore, the issue of heavy metal accumulation is of particular concern [18]. Innovative methods for processing are being developed, including the utilization of digestate in insect breeding [19]. Zheng et al. [20] utilized liquid digestate from the acidogenesis stage as a cost-effective and eco-friendly compound for the pretreatment of lignocellulosic biomass. The elevated organic carbon content of digestate is of particular significance, as it enables the production of biochar with advantageous structural properties. The transformation of digestate into biochar constitutes an innovative and promising solution for its management, consistent with the principles of a circular economy and resource recovery [21]. As indicated by reports in the literature, biochar obtained from digestate exhibits superior qualities in terms of its carbonaceous material and adsorption properties when compared with biochar produced from non-fermented biomass [22,23].

The selection of an appropriate pyrolysis temperature for digestate biochar production involves a compromise between the desired physical and chemical properties of the biochar. Changes in the structure and chemical composition of biochar can be effectively monitored using thermogravimetric analysis (TGA) and Fourier-transform infrared (FTIR) spectroscopy, respectively, while their combination (TGA–FTIR) enables the detailed identification and analysis of gases released during the thermal decomposition of biochar. These analytical techniques permit assessments of thermal stability, aromaticity, the presence and transformation of functional groups, and the nature and intensity of volatile emissions during biochar decomposition, thus facilitating the optimization of pyrolysis process parameters and consequently enabling the production of biochar with properties tailored to specific agricultural, environmental, or energy applications. Furthermore, such analyses foster a more profound understanding of the mechanisms that occur during the thermal conversion of digestates.

Despite the plethora of publications concerning the properties of biochar derived from diverse biomass types, there is a paucity of studies on digestate biochar, particularly regarding the integration of FTIR and TGA methods. Furthermore, there is a discernible absence of research focused on detailed characterization of the chemical structure and thermal stability of this type of biochar under varying pyrolysis temperatures.

The objective of this study was to evaluate the impacts of the digestate pyrolysis temperature on the structural and thermal characteristics of the resulting biochar. Particular emphasis was placed on analysis of the changes in chemical composition, the evolution of functional groups, the degree of aromatization of the carbon structure, the thermal stability, and the nature and intensity of volatile product emissions under different biochar process temperatures. The objective of this study was to ascertain the optimal pyrolysis temperature range for the production of biochar from digestate, thus yielding properties that are suited to potential environmental and agricultural applications including long-term carbon sequestration, soil improvement, and the immobilization of inorganic pollutants.

2. Materials and Methods

2.1. Digestate

The digestate was derived from an anaerobic digestion system that processed cow manure and pig manure, primarily from household sources. The fermentation process was conducted at the Bioenergia Plus facility in Piaski (in the vicinity of Lublin, Poland).

Prior to the pyrolysis process, the digestant underwent a drying procedure at a temperature of 105 °C, with the objective of achieving a constant mass. This drying process was conducted utilizing a laboratory dryer manufactured by Czylok (Jastrzębie-Zdroj, Poland). The characteristics of digestate are presented in Table 1.

Table 1. Contents of carbon, hydrogen, oxygen, nitrogen, and water forms in digestate and digestate biochar samples.

Sample	TOC	ROC	TIC	H_2O	N	C:N	H	O	Ash
				%					
Digestate	30.14	1.58	0.07	31.3	2.92	10.30	2.98	28.07	4.35
BP400	22.65	4.38	0.11	16.43	1.86	12.16	1.28	13.72	60.43
BP500	19.44	4.66	0.12	9.09	1.65	11.47	0.63	7.67	43.26
BP600	18.98	4.75	0.12	6.58	1.67	11.58	0.39	5.77	38.26
BP800	16.78	6.47	0.28	5.17	1.31	12.83	0.17	4.34	34.25

2.2. Biochar Production

Biochar was produced from dried and ground digestate by means of pyrolysis. The material was placed in a fluidized quartz reactor, which was part of a laboratory pyrolysis setup constructed at the Faculty of Chemistry, Maria Curie-Skłodowska University, Lublin, Poland.

Pyrolysis experiments were conducted in a tubular furnace (MRT-4, Czylok, Jastrzebie-Zdroj, Poland) under an inert nitrogen atmosphere with a constant gas flow rate of 20 dm^3 h^{-1}. Digestate-derived precursor samples were subjected to controlled thermal treatment using a one-step heating protocol. The material was heated from ambient temperature to the target pyrolysis temperatures of 400, 500, 600, 700, and 800 °C at a heating rate of 5 °C min^{-1} and subsequently maintained at the final temperature for 3 h to ensure complete carbonization. After cooling to room temperature under nitrogen flow, the resulting biochar was collected and labelled according to the applied pyrolysis temperature (BP400–BP800).

2.3. Determination of Carbon, Hydrogen, Moisture, and Total Nitrogen

The carbon, hydrogen, and moisture contents of the biochar were determined using a LECO RC 62 analyzer (LECO Corporation, St. Joseph, MI, USA). This instrument facilitates quantification of the total carbon and water contents, as well as the different forms of carbon—namely, organic carbon (TOC), inorganic carbon (TIC), and residual organic carbon (ROC)—based on the temperature and atmospheric conditions of the measurement, following standardized procedures for solid fuels and biomass materials (ASTM D5373-16) [24].

The total nitrogen content of the biochar samples was determined using the Kjeldahl method, in accordance with ISO 11261:1995 for organic matter analysis [25], employing a TM 8200 Foss Tecator System (FOSS, Höganäs, Sweden).

Elemental composition was determined on a dry basis. Total carbon content was calculated as the sum of TOC, ROC, and TIC. Atomic ratios (H/C and O/C) were calculated from the elemental analysis data (wt.%) by converting mass percentages to molar proportions using the respective atomic weights of H, C, and O.

2.4. Fourier-Transform Infrared Spectroscopy Analysis

The chemical structure of the biochar was analyzed via Fourier-Transform Infrared (FTIR) spectroscopy using an iS50 Nicolet spectrometer (Thermo Scientific, Waltham, MA, USA) equipped with a DTGS KBr detector. The measurements were conducted utilizing the ATR-FTIR technique, employing a diamond ATR attachment. Spectroscopic analysis was conducted within the 400–4000 cm^{-1} wavenumber range, employing a resolution of 4 cm^{-1} and accumulating 512 scans for each specimen.

2.5. Thermogravimetric Analysis

The thermal stability of the biochar was assessed by means of thermogravimetric analysis (TGA) and its derivative (DTG). Analyses were conducted over a temperature range extending from ambient temperature to 1000 °C, using a constant heating rate. Thermogravimetric analysis of the biochar was performed using a TGA55 Discovery Series analyzer (TA Instruments, New Castle, DE, USA). The measurements were conducted in an inert nitrogen (N_2) atmosphere, with a flow rate of 40 mL/min. The temperature program that was employed involved heating the sample at a rate of 10 °C/min to 900 °C, followed by an isotherm lasting 2 min. The measurement data were recorded and analyzed using the TRIOS software (version M10.1, TA Instruments, New Castle, DE, USA).

2.6. Thermogravimetric Analysis Coupled with FTIR (TGA–FTIR)

Thermal decomposition analysis of the biochar was conducted utilizing a TGA55 Discovery Series thermogravimetric analyzer (TA Instruments, New Castle, DE, USA) in conjunction with an iS50 FTIR infrared spectrometer (Thermo Scientific, Waltham, MA, USA). The mass loss was measured at various temperatures and times. The analysis was conducted in an inert nitrogen (N_2) atmosphere with a constant flow rate of 40 mL/min, thereby ensuring anaerobic conditions during measurement.

The temperature program that was employed involved heating the sample at a rate of 10 °C/min to 900 °C, followed by an isothermal hold for 2 min. Thermogravimetric data were recorded and analyzed using the TRIOS software (version M10.1, TA Instruments, New Castle, DE, USA).

The gases emitted during thermal decomposition were continuously transferred from the TGA furnace to the FTIR gas chamber via a heated transfer line. It is imperative to note that both the transfer line and the FTIR gas chamber were meticulously maintained at 250 °C to avoid the condensation of volatile products. The FTIR spectra of the gaseous decomposition products were recorded in the 400–4000 cm^{-1} wavenumber range, at a resolution of 4 cm^{-1}, with 8 scans. The analysis of the data was conducted utilizing OMNIC software (version M11.1, Thermo Scientific, Waltham, MA, USA), which facilitated the generation of 3D spectra, Gram–Schmidt curves, and chemigrams. This approach enabled the identification of functional groups as a function of time and temperature.

2.7. Thermal Stability Analysis of Biochar (TGA/DTG and FTIR)

The following indicators reflecting the thermal stability of the biochar were adopted: T_(max), R_{550}, and A/B index.

The maximum mass loss rate (T_(max)) was determined based on the DTG curves. Furthermore, the proportion of solid residue at 550 °C (R_{550}) was determined as a percentage of the initial sample mass.

The semi-quantitative A/B index—defined as the ratio of the mean absorbance in the 2970–2880 cm^{-1} range to the mean absorbance in the 1550–1600 cm^{-1} range—was calculated based on the FTIR spectra.

2.8. Use of Generative Artificial Intelligence

Generative artificial intelligence (AI) tools were used solely to assist with the translation of the manuscript text into English. The AI support was limited to language translation and linguistic clarification. No AI tools were used to generate scientific content, data, figures, analyses, interpretations, or conclusions. All scientific content and final editorial decisions were made by the authors.

3. Results

3.1. The Elemental Composition of Biochar

The elemental composition and proportions of individual carbon forms in the biochar subjected to the analyses are presented in Table 1.

As the pyrolysis temperature increased, the biochar exhibited decreasing concentrations of hydrogen, oxygen, nitrogen, and labile organic carbon while resistant organic carbon (ROC) increased, reflecting the formation of more condensed and stable carbon structures. In a previous study assessing biochar derived from sewage sludge and digestate, the carbon content increased substantially between 400 °C and 800 °C, accompanied by a clear decline in nitrogen concentration (from 1.86 to 1.3% in digestate biochar and from 4.2 to 1.36% in sewage sludge biochar) [26].

Changes in the degree of biochar carbonization were confirmed using the atomic H/C and O/C ratios shown in the van Krevelen diagram (Figure 1), which are widely applied as indicators of the stability and long-term environmental behavior of biochar [27]. With increasing pyrolysis temperature, the H/C ratio decreased markedly from 0.565 for BP400 to 0.086 for BP800, reflecting the loss of hydrogen-containing functional groups and the progressive formation of condensed aromatic structures associated with greater carbon stability [28]. As demonstrated in the study by Cayuel et al. (2015), biochar exhibiting a H/C ratio less than 0.3 has the capacity to curtail nitrous oxide emissions [18]. At the same time, the O/C ratio declined from 0.379 to 0.138 due to the removal of oxygen-containing groups through dehydration and decarboxylation reactions during thermal treatment [29]. According to the criteria proposed by Spokas et al., biochar with an O/C value between 0.2 and 0.6 can be expected to persist in the environment for 100–1000 years, whereas that with O/C below 0.2 may exhibit stability exceeding 1000 years [30]. Thus, samples BP500–BP600 can be classified as materials with medium to high durability, while BP800 represents a highly carbonized and extremely stable biochar. These findings agree with previous reports on the influences of the feedstock and temperature on biochar carbonization [30] and with the International Biochar Initiative guidelines, which indicate biochar with low O/C and H/C $\leq$ 0.6 as suitable for long-term carbon sequestration and environmental applications [31].

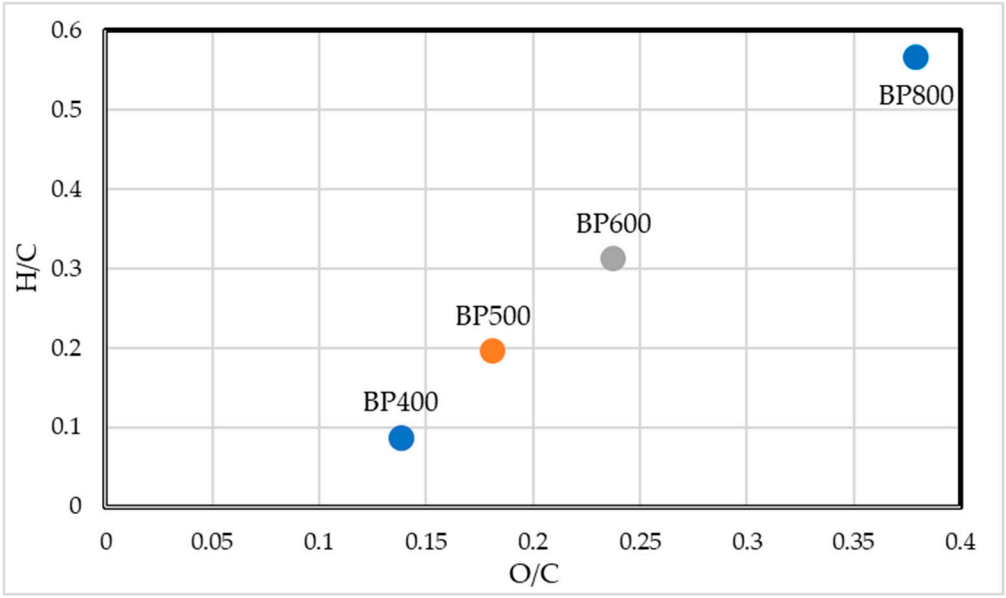

Figure 1. Van Krevelen diagram plotting atomic H/C ratio against atomic O/C ratio.

3.2. FTIR

FTIR spectroscopic studies are commonly performed to identify the functional chemical groups present in biochar and observe their changes as a function of the pyrolysis temperature [22]. Figure 2 shows the FTIR spectra of biochar obtained from pyrolysis of digestate at temperatures of 400, 500, 600 and 800 °C, while Table 2 details the assignments for the FTIR peaks.

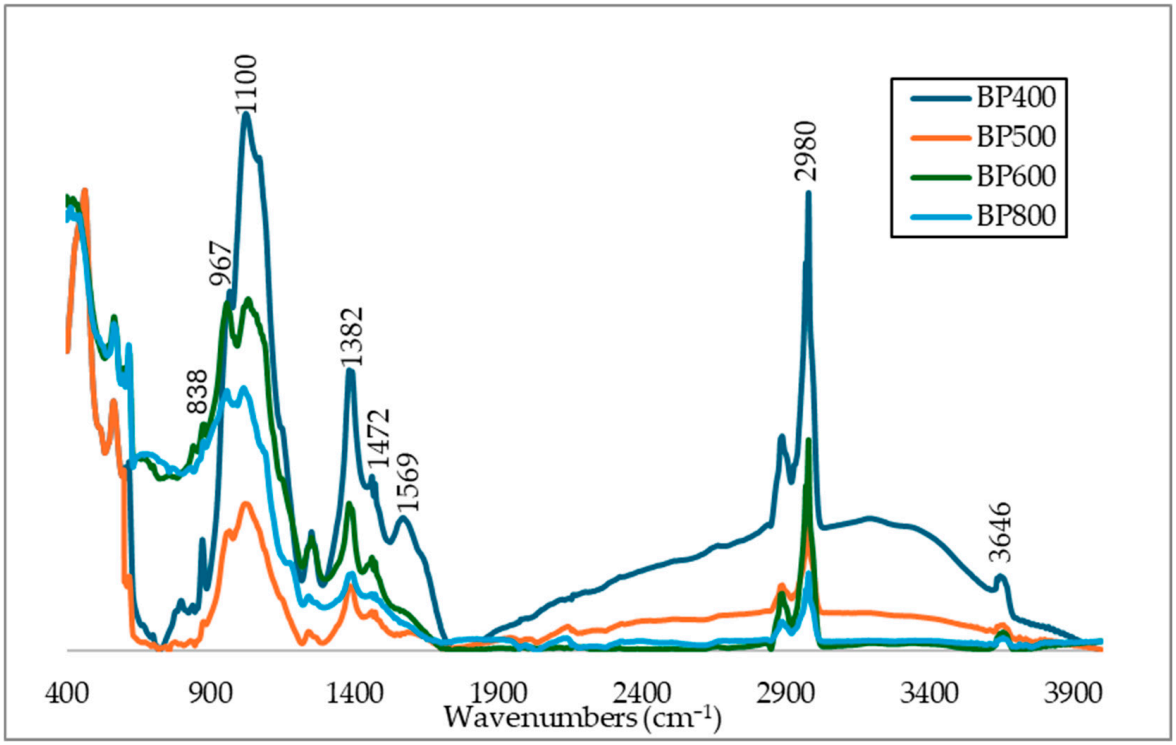

Figure 2. FTIR spectra of digestate biochar samples.

The analysis of FTIR spectra demonstrated that with an increase in pyrolysis temperature, gradual declines in the intensities of O–H bands (3600–3200 cm^{-1}) and aliphatic C–H bands (2980–2880 cm^{-1}) were observed. This finding indicates the processes of dehydration, dihydroxylation, and thermal degradation of unstable organic compounds, derived primarily from hemicellulose and cellulose or residual water [32,33]. The bands in the 2921–2851 cm^{-1} range were attributed to C–H and -CH_2 stretching vibrations, which are characteristic of aliphatic structures. The almost complete disappearance of these vibrations above the pyrolysis temperature of 600 °C confirms the decomposition of organic matter [34]. In all biochar samples examined, a band at approximately 1569 cm^{-1} was observed, corresponding to C=C vibrations in condensed aromatic structures. Notably, this band has been identified as an indicator of increasing aromatic and structural maturity in biochar [35]. In the 1200–900 cm^{-1} range, the overlap of C–O signals from organic groups with Si–O and P–O vibrations was observed, which are associated with the presence of silicates and phosphates. The bands at approximately 1350 cm^{-1} and 1384 cm^{-1} were assigned to N=O bonds and C=O vibrations of carboxyl and –OH groups of phenols, respectively [36,37]. The mineral fraction exhibited high thermal stability, and its relative share increased with the pyrolysis temperature, as confirmed by distinct bands in the 967–958 cm^{-1} range, which are characteristic of silicate and phosphate structures [38,39]. Furthermore, the bands below 900 cm^{-1}, attributed to out-of-plane C–H vibrations of aromatic rings, signify the progressive condensation of aromatic structures [40].

Table 2. FTIR peak assignments of digestate biochar samples produced at different pyrolysis temperatures.

BP400	BP500	BP600	BP800	Assignments	Compounds/Functional Groups	References
3646	3636	3636	-	ν(O–H)	Bound water, hydroxyl groups	[41]
3189	-	-	-	ν(O–H), H-bonded	Phenols, alcohols	[41]
2980	2971	-	-	ν(C–H), CH_3	Aliphatic organic compounds	[42]
2889	2889	-	-	ν(C–H), CH_2	Lipids, biomass residues	[38]
1569	1569	1569	1569	ν(C=C)	Aromatic carbon structures	[43]
-	-	-	-	ν(N–H), ν(C–N)	Amide II (proteins)	[44]
1472	1462	1462	1462	β(CO_3^{2-})	Carbonates (Ca/Mg)	[45]
1382	1382	1382	1382	ν(CO_3^{2-})	Carbonates, carboxylates	[45]
1251	-	-	-	ν(C–O)	Phenols, ethers	[46]
1100–1000	1100–1000	1100–1000	1100–1000	ν(C–O), ν(Si–O), ν(P–O)	Polysaccharides, silicates, phosphates	[39]
967	958	958	958	ν(Si–O), ν(P–O)	Silicates, phosphates	[39]
872	872	872	872	β(CO_3^{2-})	Carbonates	[45]
-	838	838	838	γ(C–H), out-of-plane	Aromatic structures	[44]
-	798	798	798	ν(Si–O)	Silicates	[39]
-	603	563	563	ν(M–O)	Metal oxides	[39]

3.3. Thermal Stability of Digestate Biochar (TGA/DTG)

The thermal stability of biochar samples obtained from digestate at temperatures of 400, 500, and 600 °C was assessed using thermogravimetric analysis and its derivatives, as demonstrated in Figures 3 and 4. It is evident that both methods facilitate the identification of temperature ranges in which thermal decomposition processes occur, in addition to providing information on the contents of volatile components, organic matter, ash, and fixed carbon [47]. The TG and DTG curves indicate a significant effect of pyrolysis temperature on the mass loss and solid residue values of the tested biochar. Consequently, the pyrolysis temperature exerts a significant influence on the extent of carbonization and the structural characteristics of the biochar. The quantitative contributions of individual stages of thermal decomposition are summarized in Table 3. It was found that only the biochar obtained at a pyrolysis temperature of 400 °C was characterized by three distinct degradation stages, which had the lowest share of solid residue. The remaining biochar samples exhibited only two stages of decomposition and a higher proportion of residues.

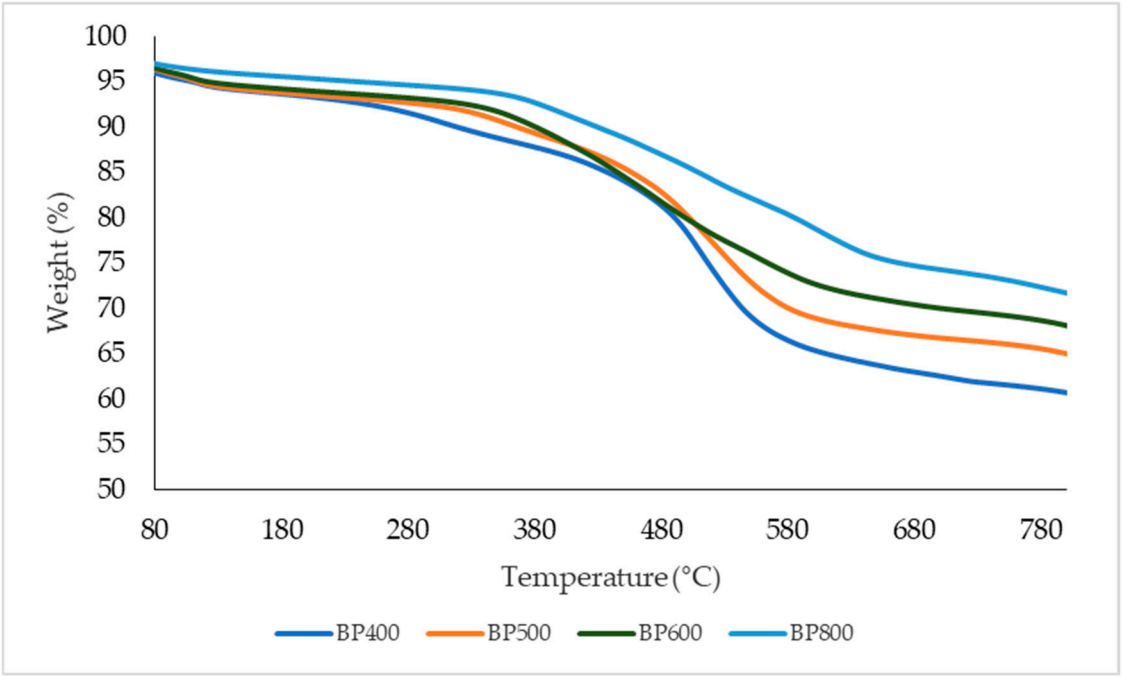

Figure 3. TGA curves for biochar samples.

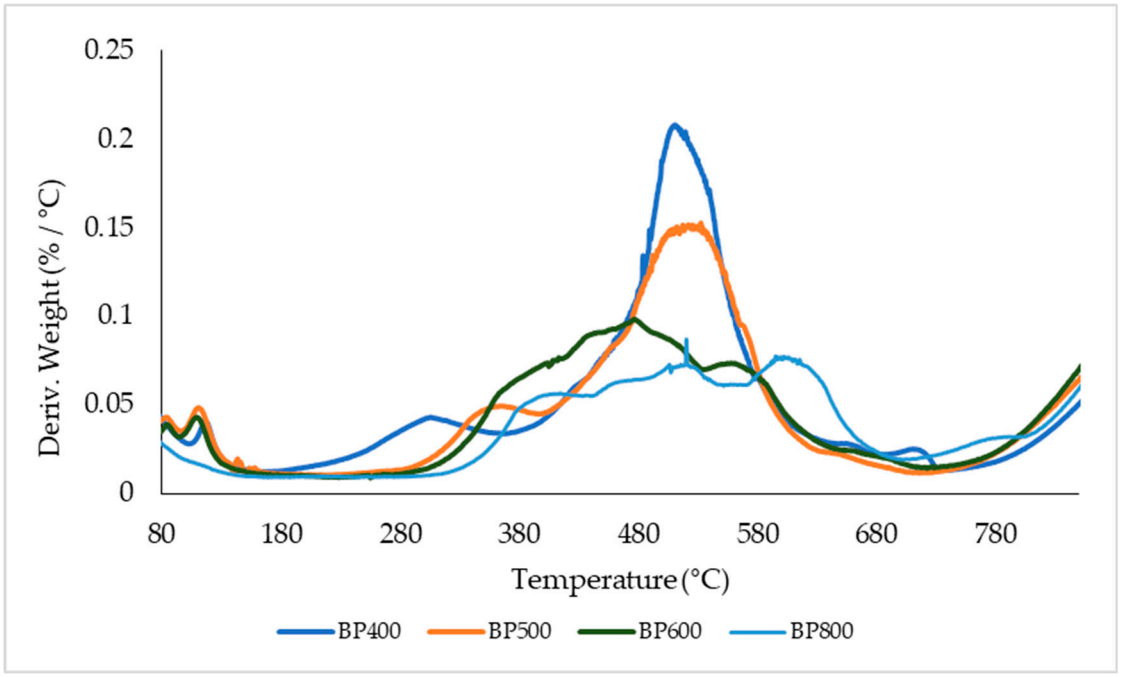

Figure 4. DTA curves for biochar samples.

Table 3. Mass loss (%) of biochar from digestate during thermal decomposition, determined via TGA/DTG.

Biochar [%]	Stage I (30–200 °C)	Stage II (200–400 °C)	Stage III (400–550 °C)	Residue (>550 °C)
BP400	5.28	5.35	24.17	61.22
BP500	4.76	25.36	-	65.68
BP600	4.95	22.47	-	69.53
BP800	3.44	19.54	-	72.28

For all biochar samples examined, the initial phase of decomposition (Stage I) occurred within a temperature range of 30–200 °C, which is predominantly attributable to the extraction of physically bound moisture and the decomposition of the most readily volatile organic compounds, which ranged from 3.44 to 5.28% and exhibited similarity across all biochar samples investigated. The values under discussion are significantly lower than those reported for raw sewage sludge, where the mass loss in this temperature range reached 6% for unfermented sludge and 10% for sludge after anaerobic digestion [37]. The limited mass loss of biochar from digestates in this temperature range serves to confirm the effectiveness of the pyrolysis process in eliminating moisture and the most labile organic fractions at the stage of biochar production.

The initial phase of mass loss (Stage II) occurred within the temperature range of 200–400 °C, which was attributed to the decomposition of less stable organic compounds, including residues of polysaccharides, lipids, and components of aliphatic structures and oxygen-containing functional groups [48].

The BP400 sample exhibited a reduced rate of mass loss in Stage II (5.35%) in comparison to the other biochar samples. This clear differentiation indicates a strong influence of the pyrolysis temperature on the distribution of thermally labile fractions in the biochar structure.

An additional decomposition stage (Stage III), spanning 400–550 °C, was only observed for biochar obtained at a pyrolysis temperature of 400 °C. The temperature range of 400–550 °C is associated with the degradation of more ordered, partially aromatic organic structures [49]. The absence of this stage in digestates pyrolyzed at 500 °C, 600 °C, and 800 °C indicates that these structures underwent further condensation during pyrolysis, leading to the formation of more stable carbon structures. It is evident that a divergence in the values obtained for biochar derived from lignocellulosic raw materials was observed.

Conversely, the share of residue above 550 °C exhibited an increase with pyrolysis temperature, reaching 61.22% for BP400, 65.68% for BP500, 69.53% for BP600, and 72.26% for BP800. The temperature range of over 550 °C pertains to the interactions of inorganic compounds, characterized by the decomposition of more stable fractions of organic matter and the degradation of certain mineral compounds. The residue resulting from this process is chiefly ash and resistant forms of carbon, which are responsible for the long-term persistence of biochar in soil [50].

The alterations in the TGA/DTG curves were corroborated by the FTIR analysis results. As the pyrolysis temperature increased, the gradual disappearance of the bands corresponding to hydroxyl groups (approximately 3636–3646 cm^{-1}) and aliphatic C–H bonds (2971–2888 cm^{-1}) was observed, which correlated with the limited mass loss in Stage I and the marked decrease in the intensity of Stage II. Concurrently, the proportion of aromatic structures increased, as evidenced by the presence of a band at around 1569 cm^{-1}, which can be attributed to C=C vibrations in aromatic rings. Bands characteristic of mineral compounds, such as phosphates, silicates, and metal–oxygen bonds, were observed in the range below 1000 cm^{-1}, indicating the presence of inorganic residues (as also observed in the TGA spectra).

3.4. Thermogravimetric Analyzer Coupled with a Fourier-Transform Infrared Spectrometer (TGA–FTIR)

The utilization of thermogravimetric analysis in conjunction with Fourier-transform infrared spectroscopy (FTIR) for the detection of gases emitted during the heating of the sample materials permitted a qualitative evaluation of the effect of the pyrolysis temperature on the nature of volatile products generated from digestates. The TG–FTIR spectra (Figure 5a–d) of the biochar samples demonstrate that with increasing pyrolysis temper-

ature, changes in both the intensity of gas emissions and the degree of carbon structure stabilization are observed.

The TGA–FTIR spectra of the BP400 biochar sample revealed strong bands attributed to CO_2 (~2350 cm^{-1}), as well as distinct signals in the 1000–1200 cm^{-1} range, which are characteristic of C–O and C-O-C bond vibrations. The presence of these bands is indicative of a significant contribution of oxygen functional groups and incomplete decomposition of organic matter. The maximum emission intensity was observed in the middle stage of the process, thereby confirming the high thermal reactivity of the biochar and the ongoing decarboxylation and devolatilization processes. This emission pattern serves to confirm that biochar obtained at a pyrolysis temperature of 400 °C represents a transitional structure between digestate and fully stabilized biochar.

It has been demonstrated that an increase in the pyrolysis temperature to 500 °C results in a substantial decrease in volatile organic compound emissions and a simplification of the gas phase composition. The TGA results indicated a two-stage mass loss, with the dominant stage being associated with the decomposition of the remaining organic structures. The TGA–FTIR spectra of the BP500 biochar sample were characterized by the predominant presence of CO_2 bands, while signals indicative of C–O bonds exhibited a substantial attenuation in comparison to the BP400 biochar. The absence of clearly defined bands corresponding to aliphatic hydrocarbons suggests progression towards carbonization and a concomitant reduction in oxygen-containing functional groups. Concurrently, the elevated level of residual carbon observed in the TGA results (Figure 4a) is indicative of the substantial mineral composition and augmented thermal stability of this biochar. As Wang et al. (2020) ([51)] previously demonstrated, an analogous phenomenon was observed in the temperature range of 450–500 °C, where a discernible decline in the intensity of the bands corresponding to the C–O and C=O groups was evident. This decline was interpreted as being due to carbonization and decomposition of the residual aliphatic structures [51]. The authors placed particular emphasis on the fact that at this stage of the pyrolysis process, the primary source of carbon dioxide is secondary reactions involving decomposition of the carbon structure and the transformation of oxygen groups associated with lignin. This finding is in alignment with the nature of the FTIR spectra obtained in this study.

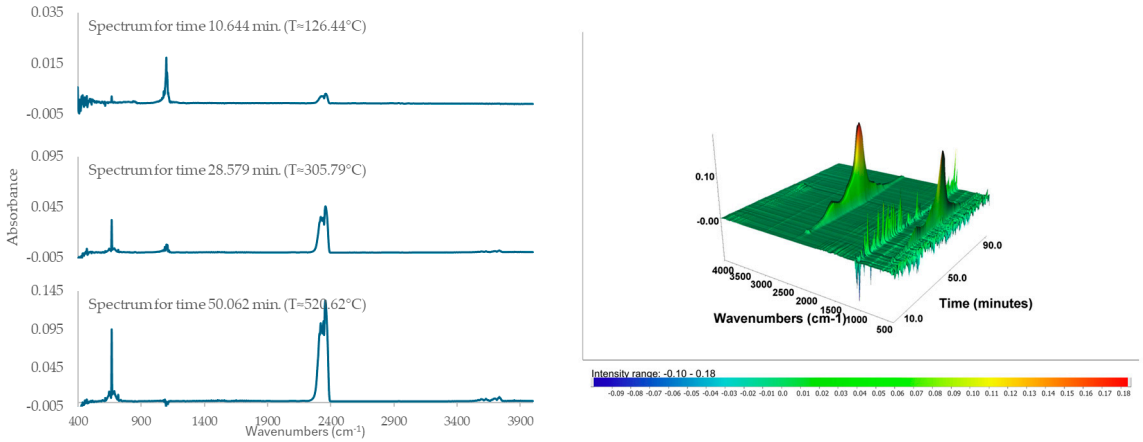

(**a**)

Figure 5. *Cont.*

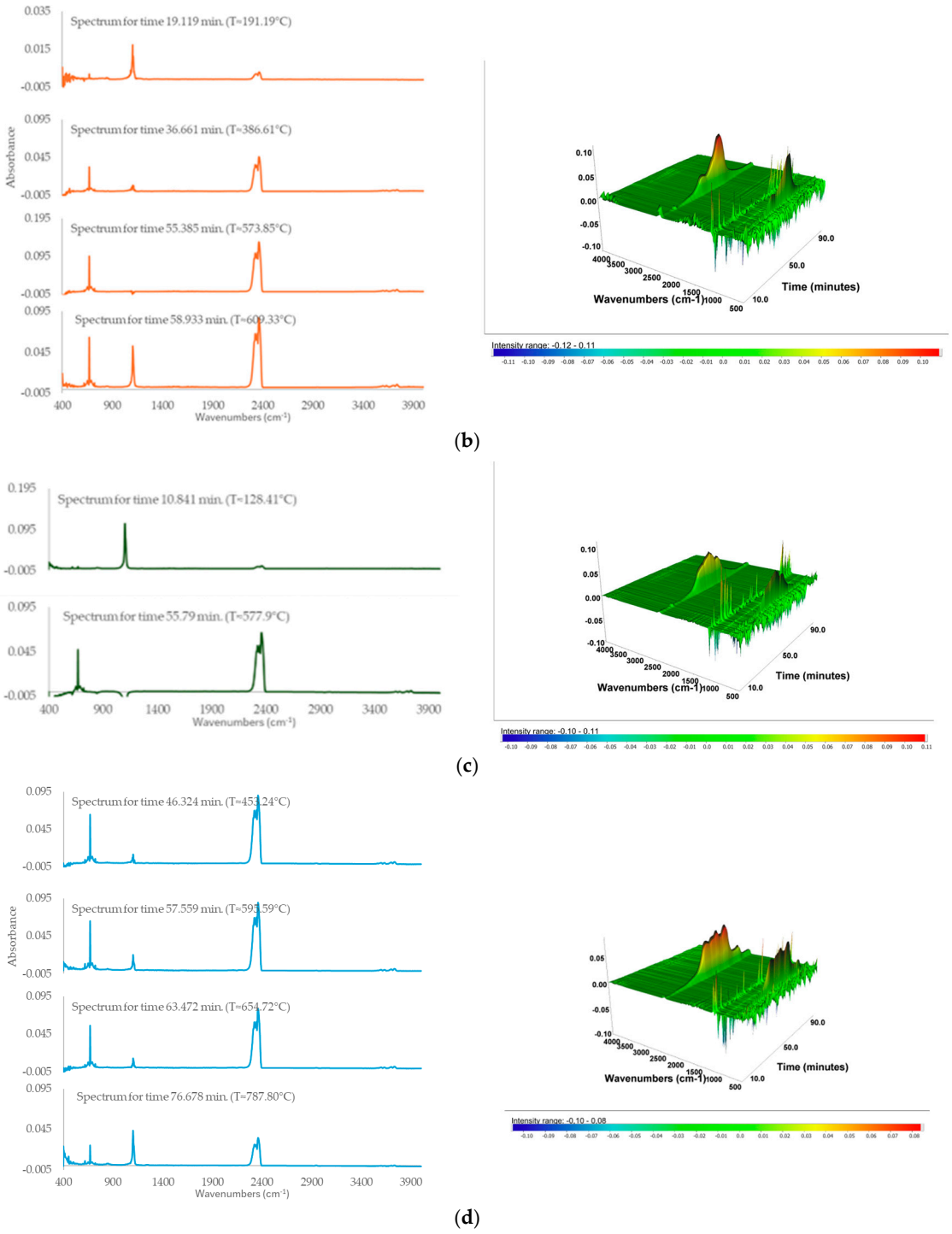

Figure 5. TGA–FTIR analysis of biochar samples: (**a**) BP400; (**b**) BP500; (**c**) BP600; (**d**) BP800.

The TGA–FTIR spectra of the BP600 and BP800 biochar samples revealed weak, short-lived signals corresponding to CO_2 emission, while the FTIR spectra recorded at different analysis times showed no significant bands originating from organic compounds. The reduced intensity of the CO_2 bands in comparison to the other biochar samples examined indicates that the majority of the reactive oxygen groups had been eliminated during the initial stages of pyrolysis. The biochar samples analyzed in this study were distinguished by a high degree of aromatization and excellent thermal stability.

Increasing the digestate pyrolysis temperature led to a gradual transition from a material rich in reactive functional groups and intensely emitting volatile products to

biochar with a high degree of carbonization and stability. In particular, the biochar obtained at a pyrolysis temperature of 400 °C was characterized by high chemical reactivity and low structural stability, while those obtained at pyrolysis temperatures of 600 °C and 800 °C exhibited minimal gas emissions and the highest thermal resistance. Meanwhile, biochar produced at a pyrolysis temperature of 500 °C represents a compromise between reactivity and stability and has been demonstrated to have significant potential for use in both environmental and technological applications.

The findings of this study demonstrate a consistent pattern with the results of previous studies conducted on pyrolyzed digestates and sludge employing the TGA–FTIR technique, indicating a gradual reduction in oxygenate emissions with increasing pyrolysis temperature. Zhang et al. (2017) demonstrated that corn digestate was characterized by lower thermal reactivity and lower emission intensity of volatile decomposition products when compared to raw biomass, which was attributed to the earlier degradation of hemicellulose and cellulose in the methane fermentation process [52]. In this study, analysis of the gas phase composition during the main pyrolysis stage revealed that carbon dioxide was the predominant component. Concurrently, the bands indicative of oxygenates (C–O, C=O) gradually diminished with increasing temperature. A similar phenomenon was observed in this study, particularly in the case of the BP500 and BP600 biochar samples.

4. Discussion

Previous studies have demonstrated that the temperature at which biochar is produced during the pyrolysis process is a key factor determining its properties. The findings of this study, derived from the integration of FTIR spectroscopy with elemental analysis and TG–DTG curves, unequivocally demonstrate that elevating the digestate pyrolysis temperature results in carbonization of the material and alterations in its chemical structure.

Biochar obtained at pyrolysis temperatures of 400–500 °C has been shown to retain a significant number of oxygen and aliphatic functional groups, indicating the persistence of residual organic compounds with high chemical reactivity. As the pyrolysis temperature increased from 600 to 800 °C, bands attributable to C=C vibrations in aromatic structures—in addition to vibrations originating from mineral compounds such as silicates, phosphates, and carbonates—were observed in the FTIR spectra of the biochar samples.

The findings regarding the FTIR spectra were fully confirmed by the elemental analysis results. The decreases in hydrogen (1.28% for BP400 to 0.17% for BP800) and oxygen (13.72% for BP400 to 4.32% for BP800) contents with increasing pyrolysis temperature, as well as the systematic reduction in H/C and O/C ratios, clearly indicate an increasing degree of condensation and aromatization of the carbon structure. The presence of mineral bands in the FTIR spectra of the BP600 and BP800 biochar samples is consistent with increases in the inorganic fraction of carbon (0.11% for BP400 to 0.28% for BP800) and more oxidation-resistant carbon (4.38% for BP400 to 6.47% for BP800).

The structural changes observed from the FTIR spectra and elemental analysis were also directly reflected in the TG-DTG curves. The BP400 biochar demonstrated the most significant mass loss within the temperature range of 400–550 °C, while the BP500 biochar exhibited the most substantial mass loss within the temperature range of 200–400 °C. This phenomenon can be attributed to the decomposition of residual organic compounds and thermally unstable functional groups. As the temperature of the pyrolysis process was increased, the proportion of residues above 550 °C also increased, indicating an increasing proportion of condensed aromatic structures and stable mineral components.

The alterations detected in the TGA/DTG curves were corroborated by the FTIR analysis outcomes. As the pyrolysis temperature increased, a gradual disappearance of the bands corresponding to hydroxyl groups (3636–3646 cm^{-1}) and aliphatic C–H bonds

(2971–2888 cm^{-1}) was observed, confirming limited mass loss in the temperature range of 30–200 °C and a marked reduction in mass loss in the temperature range of 200–400 °C. Concurrently, there was an increase in the proportion of aromatic structures, as evidenced by the presence of a band at around 1569 cm^{-1}, which can be attributed to C=C vibrations in aromatic rings. The presence of bands characteristic of mineral compounds, such as phosphates, silicates, and metal–oxygen bonds, was observed in the range below 1000 cm^{-1}, indicating the presence of inorganic residues, as observed in the TGA spectra.

The stability indicators presented in Table 4 quantitatively confirm these trends; in particular, the stability indices of biochar from digestate determined in a nitrogen (N_2) atmosphere are shown, which reflect their degree of charring and thermal stability. In an inert atmosphere (N_2), the thermal stability of biochar is best described by the T_(max) and R_{505} indices [53]. Increasing the temperature of the pyrolysis process has been shown to lead to increases in T_(max) and residual $R_{550,}$ in the order of BP400 < BP500 < BP600 < BP800. This indicates progressive condensation and aromatization of the carbon structure with increasing pyrolysis temperature. This finding is consistent with the FTIR results, which demonstrated the disappearance of the aliphatic C–H bands and an increase in the proportion of aromatic structures, as indicated by a decrease in the A/B ratio.

Table 4. Stability indices of digestate-derived biochar samples in an inert atmosphere (N_2).

Biochar	T_(max) [°C]	R_{505} [%]	A/B (FTIR)
BP400	~510	61.22	0.92
BP500	~520	65.68	0.96
BP600	~535	69.53	0.98
BP800	~594	72.28	1.00

The uniformity of all parameters unequivocally demonstrates that elevated pyrolysis temperatures promote the processes of dehydration, dehydrogenation, and aromatization, resulting in the formation of biochar with enhanced chemical stability.

Biochar obtained from digestate exhibited properties intermediate between those of lignocellulosic biochar and biochar derived from sewage sludge, resulting from the biodegradation of organic matter during anaerobic digestion and the presence of a mineral fraction in the digestate. Compared to plant biochar, digestate biochar is significantly more stable while, compared to biochar from sewage sludge, it has a more ordered aromatic structure, making it particularly useful for carbon sequestration and environmental applications. In the case of biochar from digestate, decreases in the hydrogen, oxygen, and organic carbon contents were observed with increasing pyrolysis temperature, while the proportion of resistant carbon forms increased. These changes are much milder than those observed in the case of lignocellulosic biomass, where the intensive devolatilization of cellulose, hemicellulose, and lignin leads to a significant enrichment of elemental carbon in the biochar. A study by An et al. demonstrated that an increase in the plant biomass pyrolysis temperature from 300 to 700 °C resulted in an enhancement in the carbon content of the biochar, with increases ranging from 66.8 to 82.8% for kenaf, from 51.7 to 81.2% for jute, and from 48.8 to 74.6% for ramie [54]. The van Krevelen diagram revealed a nearly linear relationship between the H/C and O/C ratios with increasing pyrolysis temperature, indicating a predictable carbonization pathway for digestates. Most classical van Krevelen diagrams documented in the extant literature refer to raw lignocellulosic biomasses, which characteristically exhibit nonlinear carbonization pathways during pyrolysis. However, digestate is defined as a biologically pretreated and partially stabilized organic material

from which readily degradable fractions have already been removed during anaerobic digestion [55].

The TGA results for the digestate biochar samples demonstrated that the BP500, BP600, and BP800 biochars exhibited an intermediate thermal character and were less reactive than biochar derived from agricultural waste. However, these biochars were found to be more susceptible to decomposition than conventional wood biochar. To provide a basis for comparison, lignocellulosic biochar obtained from pyrolysis of corn cobs and wheat straw at 400 °C was characterized by very high mass loss in the range of 200–400 °C, reaching 35–41%, respectively; in contrast, wood biochar showed much lower values of 6–8% [56]. This finding indicates that biochars BP500, BP600, and BP800 exhibit an intermediate thermal character, being less reactive than biochar derived from agricultural waste but more susceptible to decomposition than conventional wood biochar.

In the case of biochar from digestates, a very high percentage of solid residue above 550 °C (more than 60–70%) was observed, a value which significantly exceeds the typical values for plant biochar (20–30%). The FTIR spectra of the digestate biochars indicated the disappearance of hydroxyl and aliphatic groups, along with the emergence of condensed aromatic structures with increasing pyrolysis temperature and a concomitant increase in mineral compounds. TGA–FTIR analysis of digestate biochar has indicated dominant CO_2 emissions and the limited presence of volatile organic compounds [37]. The presence of a high proportion of residue is indicative of a highly advanced degree of carbonization, as well as a significant inorganic fraction, which is characteristic of materials derived from sewage sludge and digestates. Analogous trends have been observed in research on sewage sludge; in particular, following fermentation and thermal treatment, there was a marked increase in the proportion of the stable fraction and a concomitant decrease in the organic matter susceptible to decomposition within the temperature range of 200–600 °C [37].

With increasing pyrolysis temperature, the FTIR spectra of the digestate biochar samples demonstrated the disappearance of hydroxyl and aliphatic groups, along with the emergence of condensed aromatic structures accompanied by a concomitant increase in mineral compounds. Meanwhile, TGA–FTIR analysis of the digestate biochar samples indicated the dominance of CO_2 emissions and the limited presence of volatile organic compounds. Biochar produced from lignocellulosic biomass, such as wood or straw, tends to exhibit a divergent thermal decomposition pattern, particularly at lower temperatures, in comparison to biochar derived from digestate. The observed differences can be attributed primarily to the divergent chemical compositions of the raw materials—particularly the proportions of cellulose, hemicellulose, and lignin—as well as the extent of their prior biodegradation. In a study conducted by Varol & Mutlu (2023) [57], TGA–FTIR analysis of lignocellulosic biomasses—including pinecones, olive pomace, and sunflower waste—was performed. The results of this study demonstrated the presence of significant levels of aliphatic hydrocarbons and carbonyl compounds [57]. Through analysis of the TGA–FTIR spectra of peanut shell waste biomass, Mishra et al. (2025) [58] demonstrated the emission of H_2O, CO_2, CO, carbonyl compounds, ethers, and aliphatic hydrocarbons [58]. In comparison with lignocellulosic biomass, biochar derived from digestate has been shown to emit lower levels of aliphatic hydrocarbons; this phenomenon can be attributed to the earlier biodegradation of the substrate during the methane fermentation process, indicating distinct thermal decomposition mechanisms.

This characterization facilitates the evaluation of potential applications of biochar derived from digestate. It has been demonstrated that low-temperature biochar, which is characterized by an abundance of reactive functional groups and residual organic matter, tends to exhibit high surface polarity and the capacity to undergo ionic and redox interactions. This allows for their use as soil amendments that improve nutrient retention,

microbiological activity, and contaminant immobilization, as confirmed in the literature [59]. However, their diminished structural stability curtails their feasibility for use in long-term carbon sequestration. In contrast, the presence of mineral compounds and a strongly aromatic and condensed structure are the hallmarks of high-temperature biochar. These characteristics are conducive to high environmental stability, pH buffering capacity, and effective immobilization of heavy metals and other inorganic contaminants. Increasing the pyrolysis temperature was shown to enhance chemical stability whilst concomitantly inducing a decline in surface reactivity, a phenomenon that aligns with prior research [60]. This type of biochar has the potential to be utilized in the fields of soil remediation and long-term coal stabilization. Biochar produced in the 500–600 °C range exhibits a potentially desirable combination of moderate chemical reactivity and high structural stability.

The results obtained in this study also indicate the potential of the tested biochar to increase biogas production in the methane fermentation process. The FTIR spectra of low-temperature activated carbon (BP400–BP500) revealed the presence of O–H and aliphatic C–H functional groups. In addition, the TG/DTG and TG–FTIR analyses indicated higher contents of thermolabile organic fractions and oxidized volatile compounds, particularly in the case of BP400, with the results demonstrating that this biochar exhibits notable retention of residual organic matter and redox-active surface structures. In previous research, similar low-temperature biochar has been shown to promote methane production by providing additional biodegradable carbon and facilitating electron transport or direct interspecies electron transfer (DIET) via oxygen-containing and redox functional groups [61]. Conversely, biochar produced at elevated temperatures (≥600 °C) is distinguished by heightened aromatic condensation, diminished volatile content, and augmented structural stability. These phenomena primarily contribute to stabilization of the fermentation process through the adsorption of inhibitory compounds, buffering capacity, and immobilization of microbes, as opposed to direct metabolic stimulation [62]. In this context, the intermediate pyrolysis temperature range of 500–600 °C, as observed in this study, can be considered as providing a compromise between chemical reactivity and structural stability. Biochar produced within this temperature range retains a limited fraction of surface functional groups while achieving significant carbonization and thermal stability, thus providing both moderate electron transfer activity and effective stabilization of anaerobic digestion systems.

This research contributes to the existing body of knowledge regarding the effects of the pyrolysis temperature on the properties of biochar, and the findings are expected to enable more informed and safe use of biochar in agricultural and environmental practices.

5. Conclusions

This study presents an assessment of the effects of digestate pyrolysis temperature on the chemical structure, thermal stability, and thermal decomposition of the resulting biochar. The employment of FTIR, TGA, and coupled TGA–FTIR techniques was instrumental in facilitating a comprehensive identification of alterations in the carbon structure and the composition of emitted volatile products in response to variations in the process temperature. The results obtained clearly indicate that increasing the pyrolysis temperature within the range of 400–800 °C leads to progressive carbonization, aromatization, and elimination of functional groups containing oxygen and hydrogen, leading to significant increases in the thermal and environmental stability of the biochar. Biochar obtained at temperatures ranging from 500 to 600 °C has been shown to exhibit an optimal compromise between structural stability and moderate surface reactivity. In contrast, materials produced at temperatures between 600 and 800 °C are characterized by a highly condensed aromatic structure, a high proportion of mineral residues, and minimal emission of volatile

decomposition products. The coupled TGA–FTIR analysis results confirmed significant reductions in CO_2 and oxygenate emissions with increasing pyrolysis temperature, indicating advanced stabilization of the biochar's carbon structure. Concurrently, the elevated mineral composition of the digestate endows the resulting biochar with a distinct thermal characteristic when compared with lignocellulosic biochar, thereby enhancing its resilience to thermal degradation and ensuring prolonged stability.

From an environmental perspective, a pyrolysis temperature in the range of 500–800 °C can be considered optimal for converting digestate to biochar. Materials obtained under these conditions exhibit a combination of high structural stability and moderate surface reactivity, rendering them suitable for applications including carbon sequestration, soil improvement, and immobilization of inorganic pollutants.

Author Contributions: Conceptualization, J.K. and W.C.; methodology, J.K.; software, J.K.; validation, J.K., W.C. and D.S.; formal analysis, J.K.; investigation, J.K., W.C. and B.C.; resources, D.S. and W.C.; data curation, W.C.; writing—original draft preparation, J.K.; writing—review and editing, J.K., W.C. and D.S.; visualization, J.K.; supervision, B.C.; project administration, W.C.; funding acquisition, J.K. and W.C. All authors have read and agreed to the published version of the manuscript.

Funding: This research received no external funding.

Data Availability Statement: Data are contained within the article.

Conflicts of Interest: The authors declare no conflicts of interest.

References

1. Premchand, P.; Demichelis, F.; Chiaramonti, D.; Bensaid, S.; Fino, D. Biochar Production from Slow Pyrolysis of Biomass under CO_2 Atmosphere: A Review on the Effect of CO_2 Medium on Biochar Production, Characterisation, and Environmental Applications. *J. Environ. Chem. Eng.* **2023**, *11*, 110009. [CrossRef]
2. Niedziński, T.; Łabętowicz, J.; Stępień, W.; Pęczek, T. Analysis of the Use of Biochar from Organic Waste Pyrolysis in Agriculture and Environmental Protection. *J. Ecol. Eng.* **2023**, *24*, 85–98. [CrossRef]
3. Cheng, J.; Hu, S.-C.; Kang, K.; Li, X.-M.; Geng, Z.-C.; Zhu, M.-Q. The Effects of Pyrolysis Temperature and Storage Time on the Compositions and Properties of the Pyroligneous Acids Generated from Cotton Stalk Based on a Polygeneration Process. *Ind. Crops Prod.* **2021**, *161*, 113226. [CrossRef]
4. Hernandez-Mena, L.E.; Pecora, A.A.B.; Beraldo, A.L. Slow Pyrolysis of Bamboo Biomass: Analysis of Biochar Properties. *Chem. Eng. Trans.* **2014**, *37*, 115–120. [CrossRef]
5. Wijitkosum, S.; Sriburi, T. Aromaticity, Polarity, and Longevity of Biochar Derived from Disposable Bamboo Chopsticks Waste for Environmental Application. *Heliyon* **2023**, *9*, e19831. [CrossRef]
6. Zhang, X.; Zhang, P.; Yuan, X.; Li, Y.; Han, L. Effect of Pyrolysis Temperature and Correlation Analysis on the Yield and Physicochemical Properties of Crop Residue Biochar. *Bioresour. Technol.* **2020**, *296*, 122318. [CrossRef]
7. Khater, E.S.; Bahnasawy, A.; Hamouda, R.; Sabahy, A.; Abbas, W.; Morsy, O.M. Biochar Production under Different Pyrolysis Temperatures with Different Types of Agricultural Wastes. *Sci. Rep.* **2024**, *14*, 2625. [CrossRef]
8. Zhang, H.; Chen, C.; Gray, E.M.; Boyd, S.E. Effect of Feedstock and Pyrolysis Temperature on Properties of Biochar Governing End Use Efficacy. *Biomass Bioenergy* **2017**, *105*, 136–146. [CrossRef]
9. Xiao, X.; Chen, Z.; Chen, B. H/C Atomic Ratio as a Smart Linkage between Pyrolytic Temperatures, Aromatic Clusters and Sorption Properties of Biochars Derived from Diverse Precursory Materials. *Sci. Rep.* **2016**, *6*, 22644. [CrossRef]
10. Ippolito, J.A.; Cui, L.; Kammann, C.; Wrage-Mönnig, N.; Estavillo, J.M.; Fuertes-Mendizabal, T.; Cayuela, M.L.; Sigua, G.; Novak, J.; Spokas, K.; et al. Feedstock Choice, Pyrolysis Temperature and Type Influence Biochar Characteristics: A Comprehensive Meta-Data Analysis Review. *Biochar* **2020**, *2*, 421–438. [CrossRef]
11. Xu, A.; Wu, Y.-H.; Chen, Z.; Wu, G.; Wu, Q.; Ling, F.; Huang, W.E.; Hu, H.-Y. Towards the new era of wastewater treatment of China: Development history, current status, and future directions. *Water Cycle* **2020**, *1*, 80–87. [CrossRef]
12. Czekała, W.; Jasiński, T.; Grzelak, M.; Witaszek, K.; Dach, J. Biogas Plant Operation: Digestate as the Valuable Product. *Energies* **2022**, *15*, 8275. [CrossRef]
13. European Biogas Association. Anearobic Digestion, Report of March 2024. Statistical Report 2024—Preview. Available online: https://www.europeanbiogas.eu/wp-content/uploads/2024/12/EBA_stats_report_complete_241204_preview.pdf (accessed on 1 February 2026).

14. Fu, Z.; Zhao, J.; Guan, D.; Wang, Y.; Xie, J.; Zhang, H.; Sun, Y.; Zhu, J.; Guo, L. A Comprehensive Review on the Preparation of Biochar from Digestate Sources and Its Application in Environmental Pollution Remediation. *Sci. Total Environ.* **2024**, *912*, 168822. [CrossRef]
15. Herrera, A.; D'Imporzano, G.; Clagnan, E.; Pigoli, A.; Bonadei, E.; Meers, E.; Adani, F. Pig slurry management producing n mineral concentrates: A full-scale case study. *ACS Sustain. Chem. Eng.* **2023**, *11*, 7309–7322. [CrossRef] [PubMed]
16. Reuland, G.; Sigurnjak, I.; Dekker, H.; Sleutel, S.; Meers, E. Assessment of the carbon and nitrogen mineralisation of digestates elaborated from distinct feedstock profiles. *Agronomy* **2022**, *12*, 456. [CrossRef]
17. Yan, X.; Ying, Y.; Li, K.; Zhang, Q.; Wang, K. A review of mitigation technologies and management strategies for greenhouse gas and air pollutant emissions in livestock production. *J. Environ. Manag.* **2024**, *352*, 120028. [CrossRef]
18. Nayeri, D.; Mohammadi, P.; Bashardoust, P.; Eshtiaghi, N. A comprehensive review on the recent development of anaerobic sludge digestions: Performance, mechanism, operational factors, and future challenges. *Results Eng.* **2024**, *22*, 102292. [CrossRef]
19. Fu, S.-F.; Wang, D.-H.; Zhong x Zou, H.; Zheng, Y. Producing insect protein from food waste digestate via black soldier fly larvae cultivation: A promising choice for digestate disposal. *Sci. Total Environ.* **2022**, *830*, 154654. [CrossRef]
20. Zheng, H.; Tang, F.; Lin, Y.; Xu, Z.; Xie, Z.; Tian, J. Solid-state anaerobic digestion of rice straw pretreated with swine manure digested effluent. *J. Clean. Prod.* **2022**, *348*, 131252. [CrossRef]
21. Wang, X.; Wei-Chung Chang, V.; Li, Z.; Song, Y.; Li, C.; Wang, Y. Co-Pyrolysis of Sewage Sludge and Food Waste Digestate to Synergistically Improve Biochar Characteristics and Heavy Metals Immobilization. *Waste Manag.* **2022**, *141*, 231–239. [CrossRef]
22. Maroušek, J.; Minofar, B.; Maroušková, A.; Strunecký, O.; Gavurová, B. Environmental and Economic Advantages of Production and Application of Digestate Biochar. *Environ. Technol. Innov.* **2023**, *30*, 103109. [CrossRef]
23. Kończak, M.; Oleszczuk, P. Characterization of biochars produced from residues from biogas production. *J. Anal. Appl. Pyrolysis* **2015**, *115*, 157–165. [CrossRef]
24. *ASTM D5373-16*; Standard Test Methods for Instrumental Determination of Carbon, Hydrogen, and Nitrogen in Laboratory Samples of Coal and Coke. ASTM International: West Conshohocken, PA, USA, 2016.
25. *ISO 11261:1995*; Soil Quality—Determination of Total Nitrogen—Modified Kjeldahl Method. International Organization for Standardization: Geneva, Switzerland, 1995.
26. Kujawska, J.; Wojtaś, E.; Charmas, B. Biochar Derived from Sewage Sludge: The Impact of Pyrolysis Temperature on Chemical Properties and Agronomic Potential. *Sustainability* **2024**, *16*, 8225. [CrossRef]
27. Kumar, A.; Jamro, I.A.; Wang, J.; Ullah, A.; Kumari, L.; Cui, B.; Tao, J.; Guo, D.; Yan, B.; Aborisade, M.A.; et al. Co-Pyrolysis of Microalgae Residue and Sewage Sludge: An in-Depth Characterization of Kinetics, Drivers, and Gas-Oil-Char Behaviors. *J. Anal. Appl. Pyrolysis* **2024**, *179*, 106438. [CrossRef]
28. Raya-Moreno, I.; Cañizares, R.; Domene, X.; Carabassa, V.; Alcañiz, J.M. Comparing Current Chemical Methods to Assess Biochar Organic Carbon in a Mediterranean Agricultural Soil Amended with Two Different Biochars. *Sci. Total Environ.* **2017**, *598*, 604–618. [CrossRef]
29. Cayuela, M.L.; Jeffery, S.; van Zwieten, L. The Molar H:Corg Ratio of Biochar Is a Key Factor in Mitigating N_2O Emissions from Soil. *Agric. Ecosyst. Environ.* **2015**, *202*, 135–138. [CrossRef]
30. Spokas, K.A. Review of the Stability of Biochar in Soils: Predictability of O:C Molar Ratios. *Carbon Manag.* **2010**, *1*, 289–303. [CrossRef]
31. IBI International Biochar Initiative. Available online: https://biochar-international.org (accessed on 10 September 2025).
32. Bin Mobarak, M.; Pinky, N.S.; Mustafi, S.; Chowdhury, F.; Nahar, A.; Akhtar, U.S.; Quddus, M.S.; Yasmin, S.; Alam, M.A. Unveiling the Reactor Effect: A Comprehensive Characterization of Biochar Derived from Rubber Seed Shell via Pyrolysis and in-House Reactor. *RSC Adv.* **2024**, *14*, 29848–29859. [CrossRef]
33. Qu, Y.; Gandam, P.K.; Latha Chinta, M.; Gandham, A.P.; Prem, N.; Pabbathi, P.; Konakanchi, S.; Bhavanam, A.; Atchuta, S.R.; Raju Baadhe, R.; et al. A New Insight into the Composition and Physical Characteristics of Corncob-Substantiating Its Potential for Tailored Biorefinery Objectives. *Fermentation* **2022**, *8*, 704. [CrossRef]
34. Chen, L.; Wang, H.; Tu, Z.; Hu, J.; Wu, F. Renewable Fuel and Value-Added Chemicals Potential of Reed Straw Waste (RSW) by Pyrolysis: Kinetics, Thermodynamics, Products Characterization, and Biochar Application for Malachite Green Removal. *Renew. Energy* **2024**, *229*, 120724. [CrossRef]
35. Nugroho, F.G.; Ansari, A.S.; Rochman, N.T.; Khadtare, S.S.; Sree, V.G.; Shrestha, N.K.; Hafiyyan, A.F.; Im, H.; Ahmed, A.T.A. Utilizing Indonesian Empty Palm Fruit Bunches: Biochar Synthesis via Temperatures Dependent Pyrolysis. *Nanomaterials* **2025**, *15*, 50. [CrossRef] [PubMed]
36. Liu, S.; Chen, Z.; Shao, J.; Luo, S.; Yu, D. Novel Soybean Dregs Biochar Concrete: Characterization and Evaluation of the Mechanical Properties and Microstructure. *Constr. Build. Mater.* **2025**, *458*, 139512. [CrossRef]
37. Liu, C.; Ye, J.; Lin, Y.; Wu, X.; Price, G.W.; Wang, Y. Effect of Natural Aging on Biochar Physicochemical Property and Mobility of Cd (II). *Sci. Rep.* **2024**, *14*, 22214. [CrossRef]

38. Vali, N.; Zabihi, S.; Shamim, S.; Mohsenzadeh, A.; Pettersson, A. Slow-Pyrolysis of Municipal Sewage Sludge: Biochar Characteristics and Advanced Thermodynamics. *Biomass Convers. Biorefin.* **2025**, *15*, 21045–21065. [CrossRef]
39. Méndez, A.; Terradillos, M.; Gascó, G. Physicochemical and Agronomic Properties of Biochar from Sewage Sludge Pyrolysed at Different Temperatures. *J. Anal. Appl. Pyrolysis* **2013**, *102*, 124–130. [CrossRef]
40. Chatterjee, R.; Sajjadi, B.; Chen, W.Y.; Mattern, D.L.; Hammer, N.; Raman, V.; Dorris, A. Effect of Pyrolysis Temperature on PhysicoChemical Properties and Acoustic-Based Amination of Biochar for Efficient CO_2 Adsorption. *Front. Energy Res.* **2020**, *8*, 85. [CrossRef]
41. El-Sayed, S.A.; Khass, T.M.; Mostafa, M.E. Thermal Degradation Behaviour and Chemical Kinetic Characteristics of Biomass Pyrolysis Using TG/DTG/DTA Techniques. *Biomass Convers. Biorefin.* **2024**, *14*, 17779–17803. [CrossRef]
42. Alves, J.L.F.; da Silva, J.C.G.; da Silva Filho, V.F.; Alves, R.F.; de Araujo Galdino, W.V.; Andersen, S.L.F.; De Sena, R.F. Determination of the Bioenergy Potential of Brazilian Pine Fruit Shell via Pyrolysis Kinetics, Thermodynamic Study, and Evolved Gas Analysis. *BioEnergy Res.* **2019**, *12*, 168–183. [CrossRef]
43. Mekonnen, K.D. Fourier Transform Infrared Spectroscopy as a Tool for Identifying the Unique Characteristic Bands of Lipid in Oilseed Components: Confirmed via Ethiopian Indigenous Desert Date Fruit. *Heliyon* **2023**, *9*, e14699. [CrossRef] [PubMed]
44. Schott, J.A.; Do-Thanh, C.-L.; Shan, W.; Puskar, N.G.; Dai, S.; Mahurin, S.M. FTIR Investigation of the Interfacial Properties and Mechanisms of CO_2 Sorption in Porous Ionic Liquids. *Green Chem. Eng.* **2021**, *2*, 392–401. [CrossRef]
45. Jiang, J.; Gao, M.-R.; Qiu, Y.-H.; Wang, G.-S.; Liu, L.; Cai, G.-B.; Yu, S.-H. Confined Crystallization of Polycrystalline High-Magnesium Calcite from Compact Mg-ACC Precursor Tablets and Its Biological Implications. *CrystEngComm* **2011**, *13*, 952–959. [CrossRef]
46. Solano Valderrama, A.C.; Rojas De Gante, C. Traceability of Active Compounds of Essential Oils in Antimicrobial Food Packaging Using a Chemometric Method by ATR-FTIR. *Am. J. Anal. Chem.* **2017**, *8*, 726–741. [CrossRef]
47. Alves, C.T.; Peters, M.A.; Onwudili, J.A. Application of Thermogravimetric Analysis Method for the Characterisation of Products from Triglycerides during Biodiesel Production. *J. Anal. Appl. Pyrolysis* **2022**, *168*, 105766. [CrossRef]
48. Djandja, O.S.; Wang, Z.-C.; Wang, F.; Xu, Y.-P.; Duan, P.-G. Pyrolysis of Municipal Sewage Sludge for Biofuel Production: A Review. *Ind. Eng. Chem. Res.* **2020**, *59*, 16939–16956. [CrossRef]
49. Nava, K.; González, K.; Castrejón, V.; Vigueras, E.; Reyes, J.; Camacho, M.; Wang, Z.; Wang, C.; Neogi, A.; Reyes, D. From Peels and Coffee Grounds to Tunable Carbon Nanodots: Waste-Derived Biocarbon Meets Ultrafast Laser Ablation. *Nanoscale Adv.* **2025**, *7*, 7620–7637. [CrossRef] [PubMed]
50. Bolan, N.; Hoang, S.A.; Beiyuan, J.; Gupta, S.; Hou, D.; Karakoti, A.; Joseph, S.; Jung, S.; Kim, K.-H.; Kirkham, M.B.; et al. Multifunctional Applications of Biochar beyond Carbon Storage. *Int. Mater. Rev.* **2022**, *67*, 150–200. [CrossRef]
51. Wang, C.; Bi, H.; Lin, Q.; Jiang, X.; Jiang, C. Co-Pyrolysis of Sewage Sludge and Rice Husk by TG–FTIR–MS: Pyrolysis Behavior, Kinetics, and Condensable/Non-Condensable Gases Characteristics. *Renew. Energy* **2020**, *160*, 1048–1066. [CrossRef]
52. Zhang, D.; Wang, F.; Yi, W.; Li, Z.; Shen, X.; Niu, W. Comparison Study on Pyrolysis Characteristics and Kinetics of Corn Stover and Its Digestate by TG-FTIR. *Bioresources* **2017**, *12*, 8240–8254. [CrossRef]
53. Wu, L.; Ni, J.; Zhang, H.; Yu, S.; Wei, R.; Qian, W.; Chen, W.; Qi, Z. The Composition, Energy, and Carbon Stability Characteristics of Biochars Derived from Thermo-Conversion of Biomass in Air-Limitation, CO_2, and N_2 at Different Temperatures. *Waste Manag.* **2022**, *141*, 136–146. [CrossRef]
54. An, X.; Zhu, Z.; Luo, X.; Chen, C.; Liu, T.; Zou, L.; Li, S.; Liu, Y. Effects of Raw Materials and Pyrolysis Temperatures on Physicochemical Properties of Biochars Derived from Hemp Stalks. *Plants* **2025**, *14*, 2564. [CrossRef]
55. Mumme, J.; Eckervogt, L.; Pielert, J.; Diakité, M.; Rupp, F.; Kern, J. Hydrothermal Carbonization of Anaerobically Digested Maize Silage. *Bioresour. Technol.* **2011**, *102*, 9255–9926. [CrossRef]
56. Đukanović, N.; Apostolović, T.; Anojčić, J.; Mutić, S.; Marjanović Srebro, T.; Kozma, G.; Deák, C.; Maletić, S.; Beljin, J. Comparative Study of Biochar from Different Biomass Feedstocks: Toward Sustainable Resource Utilization and Environmental Applications. *Molecules* **2025**, *31*, 37. [CrossRef] [PubMed]
57. Apaydın Varol, E.; Mutlu, Ü. TGA-FTIR Analysis of Biomass Samples Based on the Thermal Decomposition Behavior of Hemicellulose, Cellulose, and Lignin. *Energies* **2023**, *16*, 3674. [CrossRef]
58. Mishra, R.K.; Chinnam, S.; Sharma, A. Thermocatalytic Pyrolysis of Low-Value Waste Biomass: Thermal Decomposition, Kinetics Behaviour, and Biochar Characterization. *Results Eng.* **2025**, *25*, 104210. [CrossRef]
59. Suresh Babu, K.K.B.; Nataraj, M.; Tayappa, M.; Vyas, Y.; Mishra, R.K.; Acharya, B. Production of Biochar from Waste Biomass Using Slow Pyrolysis: Studies of the Effect of Pyrolysis Temperature and Holding Time on Biochar Yield and Properties. *Mater. Sci. Energy Technol.* **2024**, *7*, 318–334. [CrossRef]
60. Antonangelo, J.A.; Zhang, H.; Sun, X.; Kumar, A. Physicochemical Properties and Morphology of Biochars as Affected by Feedstock Sources and Pyrolysis Temperatures. *Biochar* **2019**, *1*, 325–336. [CrossRef]

61. Nie, W.; He, S.; Lin, Y.; Cheng, J.J.; Yang, C. Functional Biochar in Enhanced Anaerobic Digestion: Synthesis, Performances, and Mechanisms. *Sci. Total Environ.* **2024**, *906*, 167681. [CrossRef]
62. Wang, W.; Nie, M.; Yan, C.; Yuan, Y.; Ju, M. Effect of Pyrolysis Temperature and Molecular Weight on Characterization of Biochar-Derived Dissolved Organic Matter from Invasive Plant and Binding Behavior with Selected Pharmaceuticals. *Environ. Pollut.* **2024**, *348*, 123867. [CrossRef] [PubMed]